



HAL
open science

The model of Particles Modes. I. A paradigm for phase synchronization in tokamak turbulence

A Ghizzo, D Del Sarto

► **To cite this version:**

A Ghizzo, D Del Sarto. The model of Particles Modes. I. A paradigm for phase synchronization in tokamak turbulence. 2022. hal-03582355

HAL Id: hal-03582355

<https://hal.univ-lorraine.fr/hal-03582355v1>

Preprint submitted on 21 Feb 2022

HAL is a multi-disciplinary open access archive for the deposit and dissemination of scientific research documents, whether they are published or not. The documents may come from teaching and research institutions in France or abroad, or from public or private research centers.

L'archive ouverte pluridisciplinaire **HAL**, est destinée au dépôt et à la diffusion de documents scientifiques de niveau recherche, publiés ou non, émanant des établissements d'enseignement et de recherche français ou étrangers, des laboratoires publics ou privés.

The model of Particles Modes. I. A paradigm for phase synchronization in tokamak turbulence.

A. Ghizzo^{1†}, D. Del Sarto¹

February 17, 2022

Address: 1: IJL- UMR 7168, Campus ARTEM, 2 allée André Guinier, BP 50840, 54011 Nancy cedex, France.

† Email address for correspondence: alain.ghizzo@univ-lorraine.fr

Abstract

Super-thermal energetic particles may alter the kinetic and resonant nature of zonal flows by leading to new types of instabilities. Here we study the effects induced by super-thermal energetic ions on trapped-ion modes (TIM) by using a reduced Hamiltonian gyrokinetic model, where both fast scales (cyclotron and bounce or transit motions) are gyro-averaged. In particular, we analyse the enhancement of resonant processes induced by energetic ions associated with nonlinear phase synchronization, in an extended version of the TIM model including circulating ions. Once an energetic particle mode is driven unstable, a rich nonlinear dynamics is observed, which encompasses a frequency chirping associated to a synchronization process driven by TIM and a transition scenario. An equivalence with the classic Kuramoto model—the paradigm describing the synchronization of a system of coupled oscillators—explains much of this phenomenology.

1 Introduction

The important role played by zonal flows (ZFs) in regulating turbulence and transport in tokamaks is now broadly accepted (see Ref [1]). Two main classes of ZFs can be identified: zero- frequency ZFs that can be described by means of fluid models of turbulence, and ZFs oscillating at high frequencies, which are named geodesic acoustic modes (GAM) [2, 3]. The former, in a fluid framework, can be shown to be related to the Reynold stress tensor, or better, to the competition between Reynolds and Maxwell tensor [20]; the latter are oscillating modes induced by the coupling of poloidal density fluctuations with the curvature drift related to the geodesic curvature of magnetic field lines in a tokamak. Zero frequency ZFs and GAMs exhibit different relaxation processes: while zero-frequency ZFs can be damped by collisions, GAMs have their own collisionless relaxation mechanism, sensitive to the Landau resonance condition.

It is nowadays well-known that also energetic particles may change the intrinsic nature of GAMs. Plasma oscillations that resonantly interact with the characteristic frequencies of fast particles (for example the transit-bounce or precession frequencies), can be driven unstable. Energetic particles, via the free energy associated with the velocity space gradient in their phase-space distribution, can thus excite a new GAM-like mode, the so-called energetic-particle-induced GAM, or “EGAM” [4, 5, 6]. Its characteristic oscillation frequency is half of ω_{GAM} .

In a similar way, the zero- frequency component of ZFs may also be modified by three-wave parametric processes. Plasma turbulence differs in many ways from fluid turbulence, and in tokamaks it is mostly driven by the free energy which is the source of many micro-instabilities that are mostly related to the gradients of density and temperature. In the core of the tokamak plasma the dominant micro-instability driving turbulence is the “ion-temperature-gradient” (ITG) mode, which concerns circulating ions. However when the frequency of ITG mode falls below the ion bounce frequency ω_{bi} , the dynamics of ions trapped in the so-called “banana-orbits” becomes more important and

one names “trapped ion modes” (TIMs) the corresponding unstable modes. In refs. [7, 8] the lower frequency range of these modes has been studied and it has been shown the existence, as a result of a parametric-like process, of a ZF oscillating at the ion precession frequency, which is well below the characteristic frequency of both GAM and EGAM.

This change in the nature of the ZF is similar to a synchronization mechanism where a phase lock appears induced by a resonance with a TIM mode. The principle of synchronization of various particle modes (here TIM and / or ZF) is not new and has already been mentioned in order to interpret some experimental results. For example, the effects of synchronization of GAMs by magnetic fluctuations were reported in [9]. This observation suggests that locking between GAMs and magnetic fluctuations can take place when their phases are shifted via a nonlinear interaction that occurs when energetic particles are injected.

Here we will approach the problem of the oscillating behavior of low-frequency ZF from the perspective of phase synchronization dynamics, by considering how the nonlinear dynamics of ZFs is modified by a small population of energetic ions. In this article, which constitutes the first of two companion articles, we show how the model of trapped particle modes, initially developed to study ITG instabilities in the very low-frequency regime [10, 12, 7, 8], can be used to develop a model of ZF-mode coupling which is based on the synchronization mechanism. To this purpose we introduce two new “particle mode” components, the co-circulating and the counter-circulating ion populations. While in the high-frequency regime synchronization processes of GAMs can be, for instance, driven by magnetic fluctuations, the situation is somewhat different in the low-frequency regime, where it is the low-frequency ZF component that can be strongly affected by synchronization processes driven by TIMs. Thus, in the low-frequency regime of ITG instabilities, another type of synchronization takes place, which is induced by trapped particle modes. The underlying physical mechanism of phase synchronization in the low frequency regime of ITG instabilities can be identified to occur through the synchronization of TIM with fast circulating ions via nonlinear, resonant wave-particle

interactions. We are here going to show how this mechanism is analogous to the synchronization of weakly coupled oscillators in the Kuramoto model (see Refs. [13, 14]). Review papers on the latter can be found in Refs. [15, 16].

The remainder of this paper is organized as follows. In sec. II, building on previous works of Refs. [7, 8], we cast wave-particle interactions in a Hamiltonian form. We so determine the Vlasov equation for each species in action-angle coordinates, by taking into account the complex precessional motion of circulating (trapped) ion populations, gyro-averaged over fast scales which correspond to the cyclotron and transit (bounce) motions. We also include trapped electrons modes (TEMs) and a small population of energetic ions: this constitutes the model of particle modes, i.e. TIMs, TEMs and co-passing and counter-passing ion modes. Note that this provides the first inclusion of energetic ions, which lead to the accounting of co-passing and counter-passing ion modes, in the action-angle model [10] which somewhere else has been named "TERESA", with reference to one of its parallel implementation [11]. We present in sec. III the main properties of the reduced Hamiltonian model in terms of linear analysis for ITG-driven instabilities. Sec. IV introduces the basic concepts of synchronization in connection with particle modes, the main difference with respect to the Kuramoto model being in the fact that the discrete and finite number of oscillators in the latter is here replaced by a spectrum of modes in the phase space, a priori. In Sec. V we discuss a numerical simulation where synchronization effects have been enhanced by the introduction of a small population of fast ions, by showing how coupling with fluid-type Kelvin-Helmholtz modes can take part in the process, too. Note that in this numerical result we focus on what we could name a "partial" synchronization process, in which only a fraction of the particle modes synchronizes via the energetic ions. We will discuss in a companion paper how the transition from a "partial" to a "global" synchronization, in which all particle modes lock to the same frequency close to the ion precession frequency, can occur if the energy density of the circulating ions trespasses some threshold value. Finally, conclusions are drawn in sec. VI.

2 The model of Trapped and Circulating Particle Modes

2.1 Hamiltonian formalism in action-angle coordinates

The Vlasov equation describing the evolution of the distribution function f_s of particles of a given species s , can be written in the form

$$\frac{\partial f_s}{\partial t} + \frac{\partial}{\partial \boldsymbol{\alpha}} (\dot{\boldsymbol{\alpha}} f_s) + \frac{\partial}{\partial \mathbf{J}} (\mathbf{j} f_s) = \frac{\partial f_s}{\partial t} + \dot{\boldsymbol{\alpha}} \frac{\partial f_s}{\partial \boldsymbol{\alpha}} + \mathbf{j} \frac{\partial f_s}{\partial \mathbf{J}} = 0, \quad (1)$$

where the Hamiltonian of the system $H_s = H_s(\mathbf{J}, \boldsymbol{\alpha}, t)$ relates the action variable \mathbf{J} and its conjugated angle variable $\boldsymbol{\alpha}$ through Hamilton equations

$$\frac{\partial H_s}{\partial \boldsymbol{\alpha}} = -\dot{\mathbf{J}} \quad \text{and} \quad \frac{\partial H_s}{\partial \mathbf{J}} = \dot{\boldsymbol{\alpha}}. \quad (2)$$

Then, assuming that the Hamiltonian at equilibrium is a function of the variables \mathbf{J} only, i.e. $H_s = H_{s,0}(\mathbf{J})$, the laws of motion can be cast in a Hamilton-Jacobi form:

$$\dot{\mathbf{J}} = 0 \quad \text{and} \quad \dot{\boldsymbol{\alpha}} = \frac{\partial H_{s,0}(\mathbf{J})}{\partial \mathbf{J}} = \boldsymbol{\Omega}(\mathbf{J}). \quad (3)$$

Even in a gyrokinetic modeling, which is based on an average over the fast cyclotron scale, it is difficult to simulate low-frequency phenomena such as micro-turbulence for time intervals as large as the confinement time. To avoid a direct treatment of a multiple hierarchy of spatial and temporal scales, a nonlinear gyrokinetic model, referred in Refs. [10] as the trapped-particle model, has been developed by making a double average over the cyclotron phase α_1 and the bounce phase α_2 (the so called ‘‘banana’’ orbit for trapped particles). This makes it possible to rule out high-frequency phenomena, so that only the precession motion is retained. This phase-angle average leads to the following system,

$$\frac{\partial H_s}{\partial J_k} = \frac{d\alpha_k}{dt} \quad \text{for } k = 1, 2, 3 \quad \text{with} \quad \left(\frac{dJ_k}{dt} \right)_{k=1,2} = 0 \quad \text{and} \quad \frac{dJ_3}{dt} \neq 0, \quad (4)$$

thanks to the fact that each adiabatic invariant reduces the dimensionality by a factor 2. In this reduced modeling, the two important variables are the toroidal canonical momentum associated to J_3 and the precession phase which we can write $\alpha_3 = \varphi - q_0\theta$ by assuming in first approximation that $\widehat{\varphi} = 0$ and $J_3 = e\psi$. For the sake of notation, hereafter we will name $\alpha \equiv \varphi - q_0\theta$. Here ψ is the poloidal flux normalized to 2π , φ is the toroidal angle, θ the poloidal angle and $q(\psi)$ the safety factor.

2.2 Dynamics of trapped particles

We now specialize the approach detailed above to identical classes of solutions of trapped particles. The approach is the same for both ions and electrons, provided that $0 \leq \kappa < 1$. For trapped particles of species s (with $s \in \{i, e\}$), the Hamiltonian takes the form

$$H = \omega_{ds}(\kappa, E_s) \psi + J_{0s}^{(t)} \phi \quad (5)$$

where $J_{0s}^{(t)}$ is a specific operator applied for trapped particle populations, which transforms the fluctuating potential term into its global gyro-average, and where $\omega_{ds}(\kappa, E_s)$ is the precession frequency. Its value is given by [18]

$$\omega_{ds}(\kappa, E_s) = \pm \frac{T_s}{T_0} \omega_{d0} \overline{\omega}_d^{(t)}(\kappa) E_s; \quad s = i, e \quad (6)$$

where $\omega_{d0} = \frac{q_0 T_0}{e_i r_0 R_0 B_0}$ is the ion precession frequency (at a given temperature T_0). Here the label “(t)” refers to trapped particles. In Eq. (5), the quantity E_s is normalized to the temperature T_s of the species s . The corresponding distribution function $\overline{f}_s = \overline{f}_{E_s, \kappa}(\psi, \alpha, t)$ obeys the reduced gyrokinetic Vlasov equation, which is given by:

$$\frac{\partial \overline{f}_s}{\partial t} + \omega_{ds}(\kappa, E_s) \frac{\partial \overline{f}_s}{\partial \alpha} + \left[J_{0s}^{(t)} \phi, \overline{f}_s \right] = \partial_\psi (D(\psi) \partial_\psi \overline{f}_s) \quad (7)$$

where at right hand side we have added a collision-related diffusion term, with the diffusion coefficient $D(\psi)$, which goes beyond Vlasov collisionless modeling but which will be used solely for numerical applications that we will discuss

later. Here $[\cdot, \cdot]$ denotes the standard Poisson bracket defined by

$$\left[J_{0s}^{(t)} \phi, \bar{f}_s \right] = \frac{\partial \left(J_{0s}^{(t)} \phi \right)}{\partial \psi} \frac{\partial \bar{f}_s}{\partial \alpha} - \frac{\partial \left(J_{0s}^{(t)} \phi \right)}{\partial \alpha} \frac{\partial \bar{f}_s}{\partial \psi} \quad (8)$$

In Eq. (6), the sign \pm corresponds to the sign of the charge (positive for ions and negative for electrons) and the normalized quantity $\bar{\omega}_d^{(t)}(\kappa)$ is given by (A.4) of Appendix A. Using Pade's approximates we express the $J_{0s}^{(t)}$ operator as:

$$J_{0s}^{(t)} \simeq \left(1 + \frac{E_s}{4} \delta_{bs}^2 \partial_\psi^2 \right) \left(1 + \frac{E_s}{4} \frac{\rho_{cs}^2}{r_0^2} \partial_\alpha^2 \right), \quad (9)$$

where $\frac{\rho_{cs}}{r_0} = \rho^* \sqrt{\frac{T_s m_s}{T_i m_i}}$ and $\rho^* = \frac{\rho_{ci}}{r_0}$. The ‘‘banana’’ scale δ_{bs} , introduced by the operator $J_{0s}^{(t)}$, corresponds to the width of the particle's trajectory in the ψ direction, while the gyro-phase average on the Larmor radius ρ_{cs} is performed along the direction of the precession angle α .

2.3 Dynamics of circulating ions

We now consider processes involving a population of co-circulating (here denoted \bar{f}_i^+) and counter-circulating ions (denoted \bar{f}_i^- respectively). These can be included in the trapped particle mode via the following reduced Vlasov equation, gyro-averaged over fast cyclotron plus transit scales and including the diffusive term used for numerical applications, which reads

$$\frac{\partial \bar{f}_i^\pm}{\partial t} + \omega_{ds}(E_i, \kappa) \frac{\partial \bar{f}_i^\pm}{\partial \alpha} + \left[J_{0s}^{(c)} \phi, \bar{f}_i^\pm \right] = \partial_\psi \left(D(\psi) \partial_\psi \bar{f}_i^\pm \right) \quad (10)$$

where,

$$\omega_{ds}(E_i, \kappa) = \frac{T_i}{T_0} \omega_{d0} \left(\bar{\omega}_d^{(c)}(\kappa) E_i + \sigma_\parallel \frac{\bar{\omega}_i^{(c)}(\kappa) \sqrt{E_i}}{q_0^2 \rho^*} \right), \quad s = \sigma_\parallel = \pm \quad (11)$$

Finally, the gyro-average operator for circulating ions reads

$$J_{0e}^{(c)} \simeq 1 + \frac{E_i}{4} (1 + \rho^{*2} \partial_\alpha^2 + \delta_{ci}^2 \partial_\psi^2) \quad (12)$$

The operator $J_{0i}^{(c)}$ corresponds to the gyro-average operator, acting on circulating ions: it therefore accounts for both the gyration and transit motion. The orbit of a circulating ion is a closed circle and the center of this circle deviates from the center of the magnetic surface by the amount $\delta_{ci} = \sqrt{\varepsilon} \delta_{bi}$.

2.4 Quasi-neutrality condition

Reduced gyrokinetic Vlasov equations for trapped ions and electrons and for circulating ions can be coupled together in a self-consistent way by using the electron neutrality condition $\delta n_e \simeq \delta n_i$ and assuming an adiabatic response for passing electrons. Hereafter, the index s will therefore run among the symbols $\{e, i, +, -\}$, with evident meaning. By introducing the fraction of trapped particles $f_p = \frac{2\sqrt{2\varepsilon}}{\pi}$, the quasi-neutrality condition reads

$$C_e (1 - f_p) (\phi - \langle \phi \rangle_\alpha) + \text{Pol. Terms} = \sum_{s=\{e,i,\pm\}} \text{sgn}(e_s) \bar{n}_s,$$

$$\text{Pol. Terms} = -f_p C_i \bar{\Delta}_i^{(t)} \phi - f_p C_e \bar{\Delta}_e^{(t)} \phi - (1 - f_p) C_i \bar{\Delta}_i^{(c)} \phi,$$

$$\text{and } \sum_{s=\{e,i,+,-\}} \text{sgn}(e_s) \bar{n}_s = f_p \bar{n}_i^{(t)} - f_p \bar{n}_e^{(t)} + \frac{1 - f_p}{2} \sum_{\sigma_\parallel = \pm 1} \bar{n}_{i,\sigma_\parallel}^{(c)} - (1 - f_p), \quad (13)$$

where $C_e = \frac{e}{T_e}$ and $C_i = \frac{e}{T_i}$. In Eq.(13), polarization effects are described by polarization terms ("Pol. Terms" in the equation). This consists of the contribution of the operator $\bar{\Delta}_s^{(t)}$ for the trapped particle population of species $s = e, i$, and of the operator $\bar{\Delta}_i^{(c)}$ for the treatment of energetic or thermal circulating ions. Their explicit expressions here are $\bar{\Delta}_s^{(t)} \simeq \frac{m_s T_s}{m_i T_i} (\rho^{*2} \partial_\alpha^2 + \delta_{bs}^2 \partial_\psi^2)$ and $\bar{\Delta}_i^{(c)} \simeq \rho^{*2} \partial_\alpha^2 + \delta_{ci}^2 \partial_\psi^2$. The electric potential ϕ defined by Eq.(13) makes it possible to couple Vlasov equations (7) for the description of ITG -driven instabilities for both classes of trapped particle modes (i.e. TIMs and TEMs)

and its corresponding equation (10) for co-circulating and counter- circulating ion modes. In Eq. (13) the smoothed densities $\bar{n}_s^{(t)}$ and $\sum_{\sigma_{\parallel}=\pm 1} \bar{n}_{i,\sigma_{\parallel}}^{(c)}$ are determined via integration of the corresponding distribution functions. Thus, for trapped and circulating particle populations, we respectively find

$$\bar{n}_s^{(t)} = \frac{2}{\sqrt{\pi}} \int_0^{+\infty} dE_s \sqrt{E_s} \int_0^1 d\kappa \kappa K(\kappa) J_{0s}^{(t)} \bar{f}_{s,\kappa,E_s}(\psi, \alpha, t) \quad (14)$$

and

$$\sum_{\sigma_{\parallel}=\pm 1} \bar{n}_{i,\sigma_{\parallel}}^{(c)} = \frac{2}{\sqrt{\pi}} \int_0^{+\infty} dE_i \sqrt{E_i} \int_1^{+\infty} d\kappa C K(\kappa^{-1}) J_{0i}^{(c)} [\bar{f}_i^+ + \bar{f}_i^-], \quad (15)$$

where the normalization constant C grants the total circulating ion density to be equal to 1.

3 Linear Analysis for thermal- energetic circulating ion modes

We now address the extension of TIM theory to circulating ion modes. We consider kinetic effects induced by two populations: thermal trapped ions and a population of fast ions of temperature T_{hot} , which can be both co- and counter-propagating. As we will see, energetic particles may have a strong influence on the global behavior of the plasma, for instance by modifying the nature of the interaction between TIM and the circulating ion populations. We expand the distribution functions in Fourier series in α ,

$$\bar{f}_i^{\pm}(\psi, \alpha, t) = F_0^{\pm}(\psi) + \sum_n \delta f_n^{\pm}(\psi) e^{i(n\alpha - \omega t)}, \quad (16)$$

and we keep for the initial circulating distribution $F_0^{\pm}(\psi)$ an expression similar to that given by (B.3), just by substituting the trapped precession frequency $\bar{\omega}_d^{(t)}(\kappa)$ with its circulating counterpart $\bar{\omega}_d^{(c)}(\kappa)$. Writing the precession fre-

quency (11) in the form

$$\omega_d^\pm(\kappa, E_i) = \frac{T_{hot}}{T_0} \omega_{d0} \left(\bar{\omega}_d^{(c)}(\kappa) E_i \pm \frac{\bar{\omega}_t^{(c)}(\kappa) \sqrt{E_i}}{q_0^2 \rho^*} \right) \quad (17)$$

we may determine the perturbed distribution functions δf_n^\pm as :

$$\delta f_n^\pm = -n e^{-E_i} \Delta \tau \frac{\omega_{d0} \frac{T_{hot}}{T_0} \left[\bar{\omega}_d^{(c)}(\kappa) \left(E_i - \frac{3}{2} \right) \pm \frac{\bar{\omega}_t(\kappa) \sqrt{E_i}}{q_0^2 \rho^*} \right]}{\omega - n \omega_d^\pm(\kappa, E_i)} J_{0i}^{(c)} \delta \phi_n \quad (18)$$

Here we do not take into account polarization terms and trapped electrons modes (circulating electrons being adiabatic). Introducing the average operator $\langle \cdot \rangle_{trapped\ ions} = \int_0^{+\infty} dE_i \sqrt{E_i} \int_0^1 d\kappa K \kappa$ for trapped ions and the operator $\langle \cdot \rangle_{passing\ ions} = \frac{2}{\sqrt{\pi}} \int_0^{+\infty} dE_i \sqrt{E_i} \int_1^{+\infty} d\kappa C K(\kappa^{-1})$ for passing ions, we obtain

$$C_e \delta \phi_n = f_p \left\langle \Delta \tau e^{-E_i} \frac{\left(\frac{3}{2} - E_i \right)}{\frac{\omega}{n \omega_{d0} \widetilde{T}_i \bar{\omega}_d^{(t)}(\kappa)} - E_i} \left(J_{0i}^{(t)} \right)^2 \delta \phi_n \right\rangle_{trapped\ ions} +$$

$$(1 - f_p) \left\langle \Delta \tau e^{-E_i} \frac{\left(\frac{3}{2} - E_i \right) \left(\frac{\omega}{n \omega_{d0} \widetilde{T}_{hot} \bar{\omega}_d^{(c)}(\kappa)} - E_i \right) - A^2}{\left(\frac{\omega}{n \omega_{d0} \widetilde{T}_{hot} \bar{\omega}_d^{(c)}(\kappa)} - E_i \right)^2 - A^2} \left(J_{0i}^{(c)} \right)^2 \delta \phi_n \right\rangle_{passing\ ions} \quad (19)$$

where $A = \frac{\bar{\omega}_t(\kappa) \sqrt{E_i}}{q_0^2 \rho^* \bar{\omega}_d^{(c)}(\kappa)}$ and E_i is normalized to the temperature of the species with respect to which the ensemble average expressed by the angular brackets is performed (T_i for trapped ions and T_{hot} for passing ions). In Eq. (19), temperatures \widetilde{T}_i and \widetilde{T}_{hot} are normalized to T_0 . It is then possible to use the analytic continuation (see Appendix B for more details) to determine the marginal solution by choosing $\frac{\omega}{n \omega_{d0} \widetilde{T}_{hot} \bar{\omega}_d^{(c)}(\kappa)} \sim \frac{3}{2}$ for the total circulating ion modes. Thus, the mean frequencies of fast ions are given by

$$\omega_{CIM} = \frac{3}{2} n \omega_{d0} \frac{T_{hot}}{T_0} \bar{\omega}_d^{(c)}(\kappa), \quad (20)$$

while the high drift frequencies, initially taken into account in the model are given by (11). We may consider that the linear modes, for both TIM/ TEM and circulating ions are given by Eqs. (6) and (11) respectively, while $\omega_{CIM} = n\omega_{d0} \frac{T_{hot}}{T_0} \overline{\omega}_d^{(c)}(\kappa) E_i$ corresponds to the local low-frequency value (for a given value of the energy) of circulating ion modes.

An example of the toroidal precession frequency $\omega_d(\kappa, E_i) = \omega_{d0} \overline{\omega}_d^{(t)}(\kappa) E_i$, corresponding to trapped ions, is plotted on the top panel in Fig. 1, while the middle panel shows the low-frequency value of the contribution of co-passing ions, i.e. $\omega_d(\kappa, E_i) = \omega_{d0} \overline{\omega}_d^{(c)}(\kappa) E_i$, (at temperature $T_{hot} \sim T_i$). Finally on the bottom panel, the function $\omega_d^+(\kappa, E_i)$ is represented for co-moving population of circulating ions. Grouping the separate contributions, for example in energy E_i and pitch- angle-like variable κ , one can evaluate the frequency domain of the mode or classes of solution of interest. An interaction can result from the structural link through which information is exchanged between ‘‘oscillators’’ (here, oscillating particle modes) of the system, each oscillator being defined by a set of physical parameters in κ and E_i .

It must be pointed out that the frequency given by (20) exhibits a similar expression to that obtained in (B.5) for trapped ion modes, by replacing the quantity $\overline{\omega}_d^{(t)}(\kappa)$ for trapped particles with $\overline{\omega}_d^{(c)}(\kappa)$. Resonant processes between TIMs and energetic co- circulating ion modes (EIM) take place when the frequencies of the two types of modes are close, i.e. when

$$\frac{T_{hot}}{T_0} \sim \frac{T_i}{T_0} \frac{\overline{\omega}_d^{(t)}(\kappa)}{\overline{\omega}_d^{(c)}(\kappa)}. \quad (21)$$

Such a result suggests that, when resonant processes between fast passing ions and TIMs take place, low frequency zonal flows can undergo a frequency shift which is similar to a synchronization between eigenmodes of oscillating particles modes.

At this step we can highlight three points on which the following discussion will focus:

- Trapped ion turbulence develops on a length scale of the order of the particle banana width δ_{bs} and on a time scale of the order of ω_{d0}^{-1} , and it can

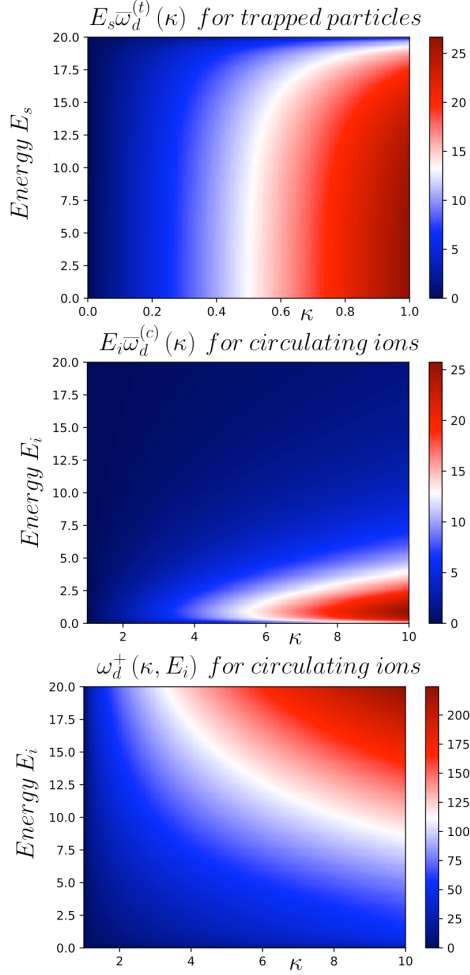


Figure 1: (Color online) Representation of the toroidal precession frequency distribution $\omega_{ds}(E_s, \kappa) = E_s \bar{\omega}_d^{(t)}(\kappa)$ in the $E_s - \kappa$ plane for trapped particles (on top panel), the corresponding (partial) precession frequency distribution $\omega_{di}(E_i, \kappa) = E_i \bar{\omega}_d^{(t)}(\kappa)$ for co-circulating ions (on middle panel) and finally of the total precession frequency distribution $\omega_{di}^+(E_i, \kappa) = \bar{\omega}_d^{(c)}(\kappa) E_i + \frac{\bar{\omega}_t(\kappa) \sqrt{E_i}}{q_0^2 \rho^*}$ for co-circulating ions (on bottom panel). In the Kumamoto model, the role of the oscillator distribution in frequency, i.e. the function $g(\omega)$ used in eq. (33) is played here by the repartition of the “frequency distribution” $\omega_{di}^+(E_i, \kappa)$ along the adiabatic invariants κ and E_i .

lead to generation of zero-frequency ZFs. Although trapped ion modes have been predicted by Kadomtsev and Pogutse fifty years ago in Ref.[18] and are well known to be subject to interchange- type instabilities, new non-trivial features can be evidenced when their hybrid fluid-kinetic nature is taken into account. Their linear frequency spectrum is then given by (B.5), which differs from the quantity $\omega_I \simeq \frac{5}{2}n\omega_{d0}\overline{\omega_d}(\kappa)$ of the (purely fluid) interchange mode.

- We note the possibility to modify the nature of zero-frequency ZFs by resonant processes which allow ZFs to oscillate at a finite frequency close to the ion precession frequency ω_{d0} , as previously shown in Ref. [7, 8]. An analogy of the latter phenomenon with synchronization processes can be established. The null frequency of the zonal mode induced by the Reynold' stress tensor associated to trapped ion turbulence is modified and becomes non-zero: this can be interpreted as due to a phase-locking mechanism, that leads to a synchronization of the ZF at the ion precession frequency ω_{d0} via resonance induced by the TIMs. This is a point on which we will focus in next Section 4.
- The frequency shift induced by phase-locking can be also interpreted in the framework of a class of fishbone-type instabilities, also called by Chen and Zonca [19, 31, 32] the "fishbone paradigm": this is characterized by the occurrence of possible resonances of the trapped particles with their precession motion. We will see, in companion paper [30], that the synchronization phenomenon involving ZFs can lead to a coupling with the toroidal mode $n = 1$. This is similar to the mode-coupling observed in fishbone instabilities involving an ideal kink mode.

4 Synchronization through resonant amplification

4.1 Basic concepts of mode synchronization and comparison with Kuramoto's model

Research on synchronization phenomena in tokamak turbulence typically focusses on ascertaining the main mechanisms responsible for collective synchronous behavior among the actors playing a role in the formation or enhancement of ZFs in the low-frequency regime. The study of the behavior of an ensemble of nonlinear oscillators weakly interacting is another scenario in which synchronization effects have been studied extensively. A simple model of such systems is the Kuramoto model (see Ref. [15]): it consists of a population of N coupled phase oscillators $\beta_n(t)$ having natural frequencies ω_n distributed with a given probability $g(\omega)$ and whose dynamics is governed by

$$\dot{\beta}_n = \omega_n + \frac{\Gamma}{N} \sum_{j=1}^N \sin(\beta_j - \beta_n) \text{ for } n = 1, \dots, N. \quad (22)$$

When the coupling is sufficiently weak, the oscillators run independently at their own frequencies ω_n . The coupling tends instead to synchronize a given oscillator to the others. In order to make a connection with the Kuramoto model, let us now consider the Vlasov equation for a population of fast ions. Using (17), the Vlasov equation (10), with no diffusion ($D = 0$) reads,

$$\frac{\partial \bar{f}_i^\pm}{\partial t} + \omega_d^\pm(\kappa, E_i) \frac{\partial \bar{f}_i^\pm}{\partial \alpha} = - \left[J_{0i}^{(c)} \phi, \bar{f}_i^\pm \right]. \quad (23)$$

Grouping the separate contributions, for example with respect to energy E_i and to the pitch- angle-like variable κ , one can evaluate the frequency domain of the mode groups or identify solution classes of interest. An interaction between these classes of solutions can result from the coupling between the associated “oscillators” (or oscillating particle modes) of the system, each oscillator being defined by a set of physical parameters that correspond to the values of κ and

E_i . An intriguing feature is that these mutual interactions can change the qualitative state of the system and can lead to a kind of mode transition via a synchronization process. Such an aspect will be presented and studied in detail in the companion paper [30].

Expressing the distribution functions in the form

$$\overline{f}_i^\pm(\psi, \alpha, t) = \sum_n f_n^\pm(\psi, t) e^{in\alpha}$$

and introducing a complex order parameter

$$\Lambda^\pm(\psi, \alpha, t) = \sum_n \Lambda_n^\pm e^{in\alpha} = - \left[J_{0i}^{(c)} \phi, \overline{f}_i^\pm \right], \quad (24)$$

Eq. (23) can be written in the Fourier space as

$$\frac{\partial f_n^\pm}{\partial t} + in\omega_d^\pm(\kappa, E_i) f_n^\pm = |\Lambda_n^\pm| e^{i\Theta_n^\pm}, \quad (25)$$

where $|\Lambda_n^\pm(\psi, t)|$ and $\Theta_n^\pm(\psi, t)$ are, respectively, the amplitude and the phase of the n -Fourier component of the complex order parameter. Therefore, the Fourier component f_n^\pm of the distribution function can be described by its (real) amplitude $|f_n^\pm|$ and by its phase $\beta_n^\pm(\psi, t)$, whose evolution satisfies the equations

$$\frac{\partial |f_n^\pm|}{\partial t} + i \frac{\partial \beta_n^\pm}{\partial t} |f_n^\pm| + in\omega_d^\pm(\kappa, E_i) |f_n^\pm| = |\Lambda_n^\pm| e^{i(\Theta_n^\pm - \beta_n^\pm)}, \quad (26)$$

or, equivalently, by separating the real and the imaginary parts:

$$\frac{\partial |f_n^\pm|}{\partial t} = |\Lambda_n^\pm| \cos(\Theta_n^\pm - \beta_n^\pm) \quad (27)$$

$$\frac{\partial \beta_n^\pm}{\partial t} = -n\omega_d^\pm(\kappa, E_i) + \frac{|\Lambda_n^\pm|}{|f_n^\pm|} \sin(\Theta_n^\pm - \beta_n^\pm). \quad (28)$$

Eqs. (27) and (28) describe the system in the form of a Kuramoto model, i.e. in terms of a population of an infinite number ($n = 1, \dots, N \rightarrow +\infty$) of coupled oscillating particle modes $\beta_n^\pm(\psi, t)$ (which play the role of ‘‘oscillators’’) having

natural frequency $\omega_n = -n\omega_d^\pm(\kappa, E_i)$ and whose dynamics is governed by

$$\dot{\beta}_n = \omega_n + \Gamma\lambda \sin(\bar{\beta} - \beta_n) \quad (29)$$

In (29) $\bar{\beta}$ plays the role of an average phase, Γ is a function defining the coupling strength and λ is a real parameter varying between zero and one, which measures the coherence of the system formed of $N \rightarrow +\infty$ oscillators. Note that in Eq.(29) there is not any label \pm , which in principle could be omitted also in Eqs.(27) and (28), provided the appropriate values of ω_n are considered. More in general, we can even extend the analysis to any type of trapped particle modes if we replace f_n^\pm with the population of the considered trapped particle species and the eigenfrequencies ω_n with the associated precession frequencies given by Eq.(6).

Eq. (29) describes a Kuramoto model in which Γ and λ are constant and a mean-field is responsible of the coupling among phase oscillators. Here the level of synchronization is conveniently measured by the order parameter $\lambda e^{i\bar{\beta}} = \frac{1}{N} \sum_{n=1}^N e^{i\beta_n}$, where the amplitude vanishes ($\lambda \rightarrow 0$) when the ‘‘oscillators’’ are out of synchrony which corresponds to incoherence and is $\lambda = 1$ in a (globally) synchronized state. Therefore, this Kuramoto-like model takes into account a partial synchronization, described by an order parameter of amplitude $0 < \lambda < 1$, and a transition from incoherence ($\lambda = 0$) to global synchronization ($\lambda = 1$).

Direct comparison of Eqs. (28) and (29) shows that the phase $\beta_n(\psi, t)$ of the Fourier component $f_n(\psi, t)$ of the distribution function corresponds to the phase $\beta_n(t)$ in the Kuramoto model. The order parameter $\Lambda_n(\psi, t) = |\Lambda_n(\psi, t)| e^{i\Theta_n(\psi, t)}$, which corresponds to $\lambda e^{i\bar{\beta}}$ in Kuramoto’s model, is determined by the Fourier component of the nonlinear Poisson bracket $-[J_0\phi, \bar{f}]_n$. This last quantity defines the nonlinear contribution to the toroidal number n from particle modes, including TIMs, and passing particle eigenmodes.

We can then define $\tilde{\Gamma} = |\Lambda_n^\pm|/|f_n^\pm|$ in Eq.(28) which replaces $\Gamma\lambda$ of Eq.(29) and accounts for both the coupling strength and the level of coherence. In the $N \rightarrow +\infty$ limit it is thus possible to introduce a critical coupling parameter $\tilde{\Gamma}_c$, with respect to which to measure the transition from incoherence to syn-

chronization that in the original Kuramoto's model only depends on λ . In the case of trapped particle turbulence, such a transition manifests as a bifurcation occurring when the critical value $\tilde{\Gamma}_c$ is attained: the “incoherence” state defined by the condition $\tilde{\Gamma} < \tilde{\Gamma}_c$ is stable because energy can not be transferred between modes and electrostatic disturbances can just decay as in the standard Landau damping scenario. When $\tilde{\Gamma} > \tilde{\Gamma}_c$, instead, only one positive eigenmode emerges from the spectrum as a consequence of synchronization, and such a bifurcation follows from the natural resonance between eigenmodes that are allowed by the system through condition (21).

4.2 Stability properties of synchronized solutions

4.2.1 Infinite $-N$ limit of the Kuramoto model

With the purpose of later applying them to the analysis developed so far, let us recall the linear stability properties of the mean-field limit of the Kuramoto model. The main idea in Kuramoto's model is to introduce, for each frequency ω , a density of oscillators $\rho(\beta; \omega, t)$ which also depends on the angle β and on the time t , and which in the limit of an infinite number of oscillators verifies the condition:

$$\frac{\partial \rho}{\partial t} + \frac{\partial}{\partial \beta}(\rho v) = 0. \quad (30)$$

This expresses the conservation of oscillators of frequency ω when the velocity $v(\beta; \omega, t)$ is given by

$$v = v(\beta; \omega, t) = \omega + \Gamma \int_0^{2\pi} d\vartheta \int_{-\infty}^{+\infty} d\omega \sin(\vartheta - \beta) \rho(\vartheta; \omega, t) g(\omega). \quad (31)$$

One can imagine each oscillator as a “particle” moving around a circle, the population of N oscillators being uniformly distributed on a circle of radius equal to 1 (i.e., with an initial probability of $\rho = \frac{1}{2\pi}$). A large cluster of synchronized oscillators appears and, with further increase of the coupling coefficient Γ , additional oscillators become synchronized while the population

behavior remains fully incoherent for sufficiently small interaction strength. A regime of (partial) synchronization, in which all oscillators with sufficiently small frequency are locked together, takes place when Γ increases beyond some threshold value Γ_c . By assuming a Taylor expansion in the form $\rho(\vartheta; \omega, t) = \frac{1}{2\pi} + \delta\rho$, the order parameter defined by $\lambda e^{i\bar{\beta}} = \int_0^{2\pi} d\vartheta \int_{-\infty}^{+\infty} d\omega g(\omega) \rho(\vartheta; \omega, t)$ reads

$$\lambda e^{i\bar{\beta}} = \int_0^{2\pi} d\vartheta \int_{-\infty}^{+\infty} d\omega g(\omega) e^{i\vartheta} \left[\frac{1}{2\pi} + \delta\rho(\omega, t) e^{i\vartheta} + c.c. \right] \quad (32)$$

and its amplitude is given by $|\lambda| = 2\pi \left| \int_{-\infty}^{+\infty} d\omega g(\omega) \delta\rho(\psi, t) \right|$. The continuity equation (30) reads

$$\frac{\partial \delta\rho}{\partial t} = -i\omega \delta\rho + \frac{\Gamma}{2} \int_{-\infty}^{+\infty} \delta\rho(\omega, t) g(\omega) d\omega, \quad (33)$$

when $g(\omega)$ is a unimodal natural frequency distribution. Strogatz et al., in Ref. [22], have shown that the incoherent solution is neutrally stable for $\Gamma < \Gamma_c = \frac{2}{\pi g(0)}$, with a linearized order parameter that decays with time. This partially synchronized state bifurcates from incoherence at $\Gamma = \Gamma_c$. In the limit of strong coupling, $\Gamma \rightarrow +\infty$ (at resonance), the ‘‘oscillators’’ become synchronized to their average phase with $\lambda \rightarrow 1$.

An analogy exists between the distribution $\rho = \rho(\beta; \omega, t)$ over natural frequencies in the Kuramoto model and the distribution function $f = f(x, v, t)$ over velocities v and space x in the one-dimensional electrostatic Vlasov model (see Appendix C). Such an analogy also exists between synchronization between oscillators (and their respective damping) and the Landau damping process in the Vlasov-Poisson system of equations. This analogy between synchronization process and Landau damping has already been introduced by S.H. Strogatz et al in [22] and more recently by S. Xu et al in [23].

Similarly to the Landau damping picture, oscillators, in the Kuramoto model, can spread out around a circle, i.e. with an angular distribution having equal probability in the interval $[0, 2\pi]$ and run, in an incoherent way, along the circle. They become well mixed by the difference in their frequencies, so that the order parameter decays to zero. Thus the damping is due to some

phase mixing phenomenon, although modified by a self-consistent decaying field. This formulation can help us to understand how the stabilization is achieved in the Hamiltonian trapped/ passing particle mode model. In the case of the trapped particle model, when the coupling among Kuramoto-like oscillators is strong enough, a fraction of them can synchronize to a common frequency close to $\omega = \frac{3}{2}n\omega_{d0} \frac{T_{hot}}{T_0} \overline{\omega_d^{(c)}}(\kappa)$ (usually with $n = 1$) and such a synchronization process can be understood as a nonlinear threshold process.

In conclusion, there are a few elements about the comparison between the Kuramoto and the trapped particle model that deserve to be put in evidence:

- In the Kuramoto model, the synchronization is realized just by phase coupling, whereas in the reduced Vlasov approach the situation is somewhat more complex, since phases in Eq.(28) and amplitudes in Eq.(27) are strongly coupled together. Therefore, resonant wave-particle interaction may force the synchronization process, a mechanism which we will study in detail in the companion paper [30] through numerical experiments.
- Within the Kuramoto-like picture of the trapped particle model, one should intuitively imagine each oscillator (or “eigenmode”) as a “particle” moving around a circle. Several resonant mechanisms among the different eigenmodes allowed by the system can be chosen: as we have done here, modes can be taken among TIMs, TEMs, low-frequency ZFs, circulating ion modes, counter-circulating ion modes or even energetic ion modes, but also hydrodynamical modes such as Kelvin- Helmholtz (KH) instabilities developing in presence of a sheared flow can be in principle considered.

4.2.2 The analogy between the Kuramoto model and energetic particle modes.

We focus on the study of energetic particle modes. Disregarding the diffusion term ($D \rightarrow 0$) and in absence of polarization effects, the basic equations of the model are

$$\frac{\partial \bar{f}_i^\pm}{\partial t} + \omega_d^\pm(\kappa, E_i) \frac{\partial \bar{f}_i^\pm}{\partial \alpha} + \left[J_{0i}^{(c)} \phi, \bar{f}_i^\pm \right] = 0, \quad (34)$$

$$C_e (1 - f_p) (\phi - \langle \phi \rangle_\alpha) = \frac{1 - f_p}{2} \sum_{\sigma_\parallel = \pm 1} \bar{n}_{i, \sigma_\parallel}^{(c)} - (1 - f_p), \quad (35)$$

where $\omega_d^\pm(\kappa, E_i)$ is defined by Eq. (17). Let us consider the distribution function of passing ions in the form $\bar{f}_i^\pm(\psi, \alpha, t) = F_0(\psi) + \sum_n \delta f_n^\pm(\psi, t) e^{in\alpha}$ and $\phi(\psi, \alpha, t) = \langle \phi \rangle_\alpha + \sum_n \delta \phi_n(\psi, t) e^{in\alpha}$. A linear analysis leads to

$$\frac{\partial \delta f_n^\pm}{\partial t} + in\omega_d^\pm(\kappa, E_i) \delta f_n^\pm - in\delta \phi_n(\psi, t) \frac{dF_0}{d\psi} = 0, \quad (36)$$

$$C_e (1 - f_p) \delta \phi_n = \frac{1 - f_p}{2} \langle \delta f_n^+ + \delta f_n^- \rangle_{\text{passing ions}}, \quad (37)$$

or, equivalently, by replacing the expression of $\delta \phi_n$ given by Eq. (37) into (36), we obtain

$$\begin{aligned} \frac{\partial \delta f_n^\pm}{\partial t} &= -in\omega_d^\pm(\kappa, E_i) \delta f_n^\pm + \\ &\frac{in}{2C_e} \frac{dF_0}{d\psi} \frac{2}{\sqrt{\pi}} \int_0^{+\infty} dE_i \sqrt{E_i} \int_1^{+\infty} d\kappa CK(\kappa^{-1}) (\delta f_n^+ + \delta f_n^-). \end{aligned} \quad (38)$$

Comparison between (33) and (38) shows that the role of $g(\omega)$ is played by the way the oscillators are distributed among the adiabatic invariants κ and E_i .

5 Numerical simulation

We now discuss some numerical results, obtained with a semi-Lagrangian technique [26, 27] that integrates the reduced Vlasov equations along their characteristics. We thus provide a quantitative example of synchronization related to the coupling between TIM and a population of fast circulating ions in presence of a sheared flow, which in turn allows the onset of a Kelvin-Helmholtz

instability that takes part in the nonlinear coupling. Details on the numerical scheme may be found in Refs. [10, 12].

5.1 Initial distribution function

We consider the reduced Hamiltonian model given by Eqs. (7), (10) coupled in a self-consistent and nonlinear way with the quasi-neutrality condition (13) initiated in a normalized equilibrium state given by

$$f_s(\psi, \alpha, t = 0) = F_{0s}(E_s) \left[1 + \omega_{ds}(E_s, \kappa) \left| E_s - \frac{3}{2} \right| \Delta\tau G(\psi) \right. \\ \left. + \delta_{tp} \left| E_s - \frac{5}{2} \right| \phi_{max} \sin 2\pi\psi \right] \quad (39)$$

with a perturbation given by

$$\delta f_s = F_{0s}(E_s) \delta\phi_{pert} \sin(\pi\psi) \cos(10\alpha). \quad (40)$$

Note that here we have used the symbol E_s for $s = e, i, b, \pm$, where we explicitly include the contributions also of the energetic ions (label "b", for "beam"). The equilibrium distribution corresponds to $F_{0s} = e^{-E_s}$ except for the co-passing ion population for which $F_{0,+} = e^{-E_i} (1 - n_b) + n_b e^{-(\sqrt{E_i} - \sqrt{E_b})^2}$. This takes into account a small population of fast co-circulating ions with density n_b , the ion beam having average energy E_b . Here $\delta_{tp} = 1$ for trapped particles and $\delta_{tp} = 0$ for passing ions. In the numerical simulations we choose $G(\psi) = \psi + \delta_{tp} \left(\frac{\sin 4\pi\psi}{8\pi} - \frac{\psi}{2} \right)$ in Eq. (39). The reason for introducing the function $G(\psi)$ and the term $\phi_{max} \sin \pi\psi$ on the right hand side of (39) is to take into account an initial shear flow in the dynamics. This shear flow gives rise to a Kelvin-Helmholtz instability. It must be pointed out that all eigenmodes introduced in simulation exhibit the same eigenfunction of the form $\sim \sin \pi\psi$. This perturbation is compatible with a number of modes and instabilities that can develop in the system: ITG modes for circulating ions, beam-plasma instabilities with the introduction of a beam of fast ions, TIMs and TEMs when trapped species are included, but also shear modes driven by the Kelvin-

Helmholtz instability (see Refs. [7, 8] for more details).

In numerical simulations the time is normalized to the inverse drift frequency $\omega_{d0}^{-1} = \frac{eB_0r_0R_0}{q_0T_0}$ and the poloidal flux ψ is given in $\Delta\psi = \frac{r_0R_0B_0}{q_0}$ units. The electric potential ϕ , together with the constants C_e and C_i , are expressed in $\omega_{d0}\Delta\psi$ units. The toroidal precession frequencies, denoted here by $\omega_{ds}(E_s, \kappa)$, are defined by eqs. (6) and (11), where $s = i, e, \pm$ for trapped ions, trapped electrons, co-passing ions (+) and counter-passing ions (-), respectively. In order to provide an efficient dissipation mechanism for the turbulence cascade, in numerical simulations we have chosen the coefficient D at right hand side of Eq.(10) to be different from zero in the vicinity of the boundary conditions of the ψ interval. In particular, we take $D \simeq 0.001$ close to $\psi = 0$ and to $\psi = 1$, in a domain extension which is less than 5% of the whole interval, whereas it is strictly to zero everywhere else. We have run a simulation with a normalized temperature gradient of $\Delta\tau = \frac{\Delta\psi}{T_i} \frac{dT_i}{d\psi} = 0.70$, chosen well above the different thresholds of ITG instabilities which are close to $\Delta\tau_{threshold} \sim C_e = 0.40$. Temperature gradients have been included for both ion and electrons and for $s = i, e, \pm$. Each species has identical banana width, $\delta_{bs} = 0.10$ (in $\Delta\psi$ units). This corresponds to $\delta_{ci} = 0.10$ for passing ions, to a Larmor radius of $\rho_{cs} = 0.01$ (in $\Delta\psi$ units) for each species, and to a magnetic shear of $s_0 = \frac{r_0}{q_0} \left(\frac{dq}{dr} \right)_{r_0} = 0.8$. The perturbation $\delta\phi_{pert}$ of Eq.(40) is chosen to have an amplitude 0.025 on the mode $n = 5$.

Preliminary results, reported in Refs. [7, 8], have shown the possibility to separately excite:

- The KH instability, by introducing in the initial equilibrium the quantity $F_{eq} = e^{-E_i} \left(1 + \left| E_i - \frac{5}{2} \right| C_i 2\pi\phi_0(\psi) \delta_{bi}^2 \right)$. This allows us to define in a self-consistent way the initial density $n_{eq}(\psi) = \sin 2\pi\psi$ (or equivalently an initial velocity shear $\phi_0(\psi) = \frac{\phi_{max}}{2\pi} \sin 2\pi\psi$) and an ion pressure $P_0(\psi) = n_0T_0 = const$ at equilibrium.
- The ITG- driven TIM instability by considering the distribution function $F_{eq} = e^{-E_i} \left(1 + \left| E_i - \frac{5}{2} \right| \overline{\omega_d^{(t)}}(\kappa) \Delta\tau\psi \right)$ (with the associated potential $\phi_0(\psi) = \frac{3}{2}\psi$).

The simulation has been initialized: by choosing $T_i = T_e = T_0$ for both ion and electron temperatures; by selecting a beam of fast ions only for the co-passing population, for which we choose $E_b = 5T_0$ and $n_b = 15\%$ of the total density; and by fixing $C_i \simeq 0.60$ for the polarization term, so that a strong coupling with the shear flow could be excited when the amplitude ϕ_{max} differs from zero. To this purpose we have taken $\phi_{max} = 0.50$ in $\omega_{d0}\Delta\psi$ units. We have used a time step $\Delta t\omega_{d0} = 0.005$ and a phase-space sampling of $N_\alpha N_\psi = 1025 \times 257$ for $N_\kappa N_E = 16 \times 120$ different Vlasov equations, which are coupled together by the quasi-neutrality condition.

5.2 Synchronous states driven by trapped ion modes

We can then address the problem of the nonlinear interaction of turbulence induced by TIMs with energetic co-passing ions, in the framework of a (partial) synchronization process. The interaction results from the coupling provided by the electric potential through the quasi-neutrality condition, by means of which information is exchanged between TIMs and the other particle modes. Here the synchronization consists in an adjustment of the phase-space dynamics of oscillator-like particle modes, which is caused by their resonant interaction.

We note that the phase-space dynamics related to the synchronization process we are interested in, can be investigated and quantified in terms of the variation of the L^2 -norm: in a recent paper [29] we have indeed shown that the net momentum transfer that can take place between coherent structures in the phase-space during, e.g., the nonlinear dynamics of some instability, can be related to an “entropy” production rate.

We can thus investigate the effects induced by the ITG turbulence due to trapped modes on other “particles modes”, as for instance co-circulating and counter-circulating ion modes, by examining the diagnostics presented in Fig. 2, which presents the time evolution of the L^2 -norm (sometimes called the “phasesrophy” in [28]) for the different modes. Although the entropy $S = \langle f \ln f \rangle$ and the L^2 -norm, defined as $S_2 = \langle f^2 \rangle$, are exact invariants in the Vlasov formalism, their invariance is only guaranteed in the sense of

the weak convergence and it is well known that physical coarse-graining or numerical effects due to the introduction of an elementary numerical cell of finite size, may lead to small variations of these quantities. Because the concept of phasestrophy is directly connected to the production and to the transfer of momentum in plasmas (see [28, 29] for more details), its variation is usually associated to the generation and growth of coherent structures, such as clump-hole pair in phase-space.

Fig. 2 shows the quantities: $S_2 = \langle f_s^2 \rangle$ versus time, where the average $\langle \cdot \rangle$ is made over the phase α (i.e. $\int_0^{2\pi} \frac{d\alpha}{2\pi}$.); the poloidal flux ψ ($\int_0^1 d\psi$.); the pitch angle κ (depending on the type of particles, trapped or circulating); and energy E_s ($\frac{2}{\sqrt{\pi}} \int_0^{+\infty} dE_i \sqrt{E_i}$.). The phasestrophy of trapped ions is plotted on top panel, while the middle and bottom panels correspond to the co-circulating and counter-circulating ion distributions, respectively. While the circulating ion modes exhibits a slow increase in time (linked to a good numerical conservation of S_2 within 2%), the dynamics of the trapped ion mode is characterized by the emergence of strong bursts, associated to the generation of a large vorticity in the phase-space (as can be seen in Figs. 4 in sec. 5.3). The relative variation of $S_2(f_{trapped})$ is close to $\Delta S_2 = (S_2(t) - S_2(0)) / S_2(0) = (1.1 - 0.4) / 0.4 \sim 175\%$ for trapped ions, and of $\Delta S_2 = (0.000332 - 0.000325) / 0.000325 \sim 2.15\%$ for co-passing ions (and of 1.15% for counter-passing ions). This clearly indicates that in this scenario the TIM drives the turbulence and acts as a “pump” mode. The overall result can be interpreted as a synchronization process in which only a fraction of the particle modes has locked to the frequency $\omega = \frac{3}{2} \omega_{d0} \overline{\omega_d}^{(c)}(\kappa)$. The fact that only a fraction of particle modes has underwent synchronization is visible from Figs. 5 (see below), where a downward shift in frequency is observed.

Because of this reason we call it "partial synchronization", in contrast with the condition of "global" synchronization, which we will speak of, and give proof of, in the companion paper [30]. Here we want to put emphasis on, and provide a proof of concept of the synchronization mechanism itself, in which, as discussed before (second "bullet point" in Sec.4.2.1), also further modes like KH-type modes can take part. In order to better characterize this

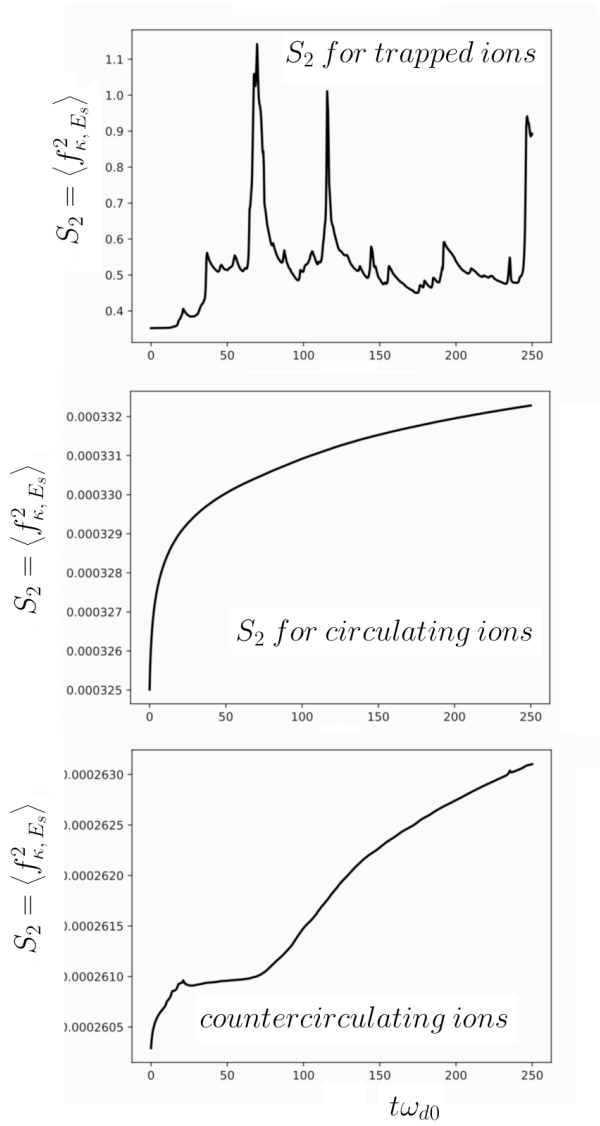


Figure 2: Time evolution of the L^2 -norm $S_2 = \langle f^2 \rangle_{\alpha, \psi, \kappa, E_s}$ for trapped-ion modes (TIM) (on top panel), for co-circulating ion mode (on middle panel) and finally of the counter-circulating ion mode (on bottom panel). The concept of “phasesrophy” is usually associated to the momentum transfer in plasma, in link with the formation and displacement of vortex structures such as the clump-hole pair creation predicted in the Berk- Breizman model for instance. We observe that only TIM on top panel exhibits a bursting behavior with strong peaks associated to the emergence of coherent structures in phase space, which indicates that TIM is the “pump” particle mode, while the other modes are indeed synchronized states, which shows a very well conservation of the phasesrophy.

process as a Kuramoto-like synchronization, we also underline that the chirped frequency, close to $\omega \sim 0.5\omega_{d0}$, is observed well below the values expected from linear theory (shown in Fig. 1), which indeed are 400 times higher (bottom panel in Fig. 1).

Previous analysis has shown that it is the term $\Lambda_s(\psi, \alpha, t) = - \left[J_{0i}^{(c)} \phi, \overline{f_s} \right]$ that plays the role of the order parameter λ in the Kuramoto model. Even without explicitly evaluating the Poisson bracket, it is possible to obtain information on how the synchronization process is realized by looking at the dominant term in the Poisson bracket of Eq. (24), that is, the contribution of $\left\langle \frac{\partial J_{0s} \phi}{\partial \psi} \overline{f_s} \right\rangle$, the average being made over all variables κ , E_s , ψ and α . The frequency spectrum of $\left\langle \frac{\partial J_{0s} \phi}{\partial \psi} \overline{f_s} \right\rangle$ for trapped and co-passing ions is plotted in Fig. 3 on top and bottom panel, respectively. The zoom of the spectrum on the top panel clearly indicates that the turbulence is produced in a very low-frequency regime, close to $\omega \sim 0.90\omega_{d0}$. The frequency locking is another important evidence to prove the synchronization of (thermal plus fast) co-passing ions: it can be seen on bottom panel in Fig. 3, which exhibits a similar dominant peak to that of top panel.

5.3 Phase space dynamics.

The whole picture of the plasma dynamics, given in Figs. 2 and 3, is completed by analyzing the behavior of the trapped ion distribution shown in Fig. 4 at four different times. The first burst in the phasestrophy S_2 at time $t\omega_{d0} \simeq 70 - 80$ (shown in Fig. 2 on top panel) is accompanied by the emergence of four trapping structures driven by the TIM turbulence in the $\psi - \alpha$ phase plane, which are shown on the top left panel of Fig. 5. A major role in the interaction is played by the KH-driven shear flow at time $t\omega_{d0} \sim 120$ (top right panel in Fig. 4), this burst in activity being linked to the emergence of the second peak in the dynamics of S_2 for trapped ions (shown in the top panel in Fig. 2).

The increase of the turbulent energy is linked to the formation and growth of vortices in the trapped ion distribution function, corresponding to the

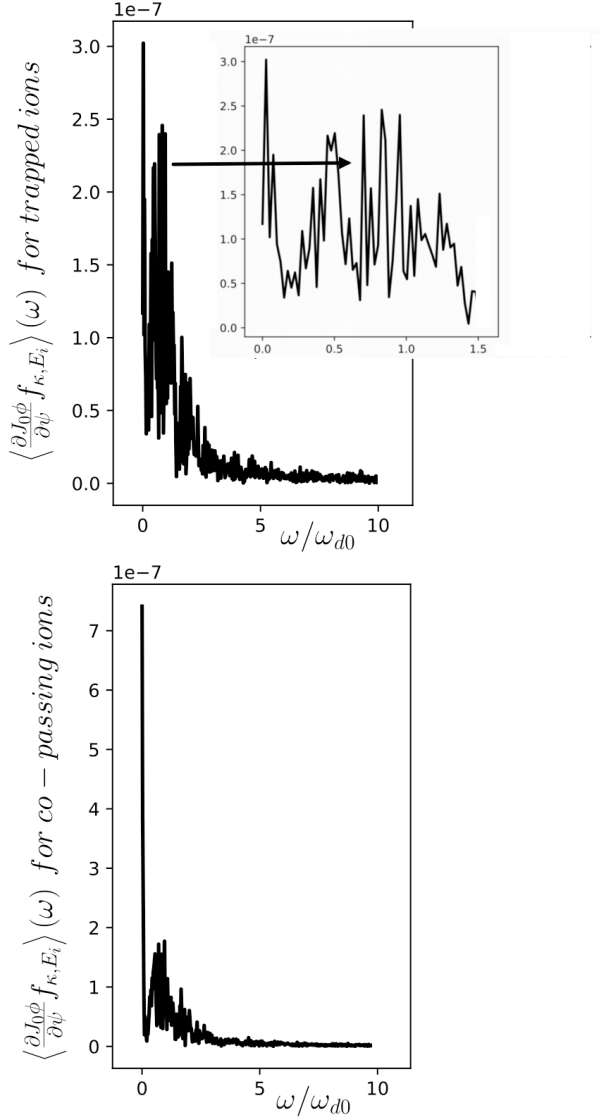


Figure 3: The spectrum of $\langle \frac{\partial J_{0s}\phi}{\partial \psi} \overline{f_s} \rangle (\omega)$ in frequency for trapped ions is plotted on top panel while the corresponding spectrum for copassing ions is plotted on bottom panel. A zoom, illustrating the behavior of the spectrum in the range of small frequencies has been added on top panel. The synchronization mechanism or frequency entrainment is clearly observed for (thermal plus fast) copassing ions, driven by the “pump” particle mode (TIM) , shown on top panel.

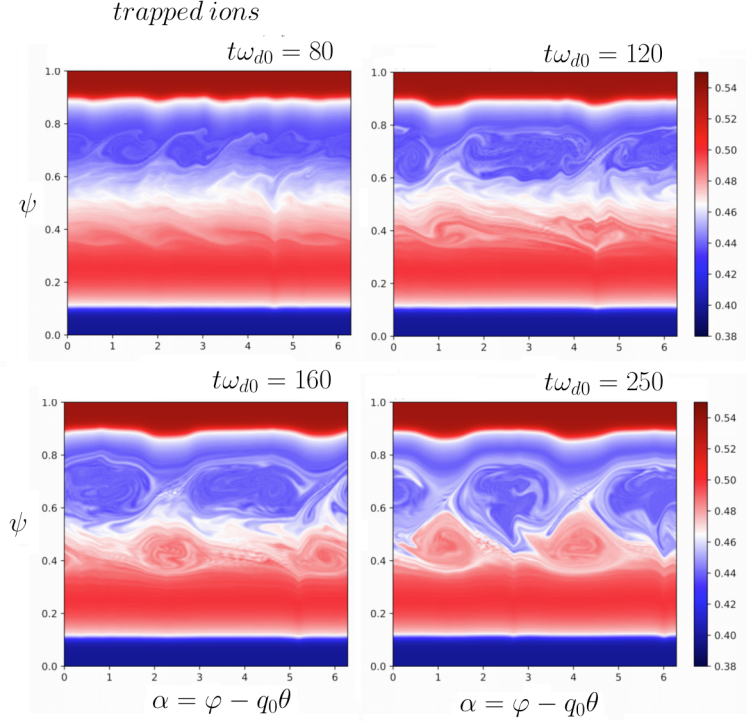


Figure 4: (Color online) Representation of the trapped ion distribution in the $\psi - \alpha$ phase space at four different times. The first burst in the phasestrophy S_2 at time $t\omega_{d0} \simeq 70 - 80$ (shown in Fig. 2 on top panel) is accompanied by the emergence of a four-trapping structures in the $\psi - \alpha$ phase driven by the TIM turbulence (on the top left panel). A reorganization takes place associated to the emergence, at time $t\omega_{d0} \sim 120$, (on top right panel), of a sine-type vortex structure, on the toroidal number $n = 2$, driven by the shear flow.

toroidal mode number $n = 4$ at time $t\omega_{d0} = 80$, followed by a re-organization of the plasma that corresponds to the emergence of a sine-type perturbation in density on the toroidal mode $n = 2$ at time $t\omega_{d0} = 120$; the latter is driven by the KH instability. Such a sine-type structure differs from the usual hole clump pair creation [33, 34, 35], usually observed in the so-called “bump-on-tail” paradigm, which is in turn typically associated to strong frequency sweeping.

Fig. 5 shows the frequency spectrum of the quantity $\left\langle E_i \frac{\partial J_{0i}\phi}{\partial \alpha} \frac{\partial \bar{f}_i}{\partial \psi} \right\rangle$, the first moment with respect to the ion energy E_i of the $\frac{\partial J_{0i}\phi}{\partial \alpha} \frac{\partial \bar{f}_i}{\partial \psi}$; again, the average $\langle \cdot \rangle$ is performed with respect to all variables κ , E_s , ψ and α . This function gives an estimation of the order parameter $\langle \Lambda_s(\psi, \alpha, t) \rangle_{\psi, \alpha}$ in the synchronization mechanism induced by the “pump” driver term (the trapped ion population, shown on top panel) and another particle mode (the co-circulating ion population shown in bottom panel in Fig. 5). On top panel, we have plotted the spectrum in frequency of this quantity for TIM: we observe that the spectrum lies in the range from 0 to $12\omega_{d0}$, corresponding to a large frequency spread of TIMs driven by the coupling with the shear flow and energetic ions. During the saturation of the KH instability, nonlinear sine-type vorticities are formed and such structures are produced by strong density fluctuations that can lead to the destabilization of TIMs by modifying nonlinearly the gradients in density and temperature. The frequencies corresponding to the toroidal numbers $n = 4$ and $n = 2$, which are visible in Figs. 4, are evidenced by arrows in the figure. We see that a TIM-like hole structure tends to lower its own energy due to the presence of shear flows (dominant, in the standard fluid model, in the regime where $E_i \sim 0$) and because of the energy dependence of the toroidal precession frequency of banana-orbits, $\omega \sim n\omega_{d0}\bar{\omega}_d(\kappa) E_i$, its frequency must decrease. As a consequence one measures a downward chirping of the frequency of TIMs (evidenced in the figure by the word “chirped”), similar to the behavior of fishbone modes in tokamaks.

The frequency spectrum shown in bottom panel of Fig. 5 for the co-passing ion distribution can be interpreted as a synchronization between the co-passing ion mode and the “chirped” resonance frequency of the $n = 1$ TIM. The latter

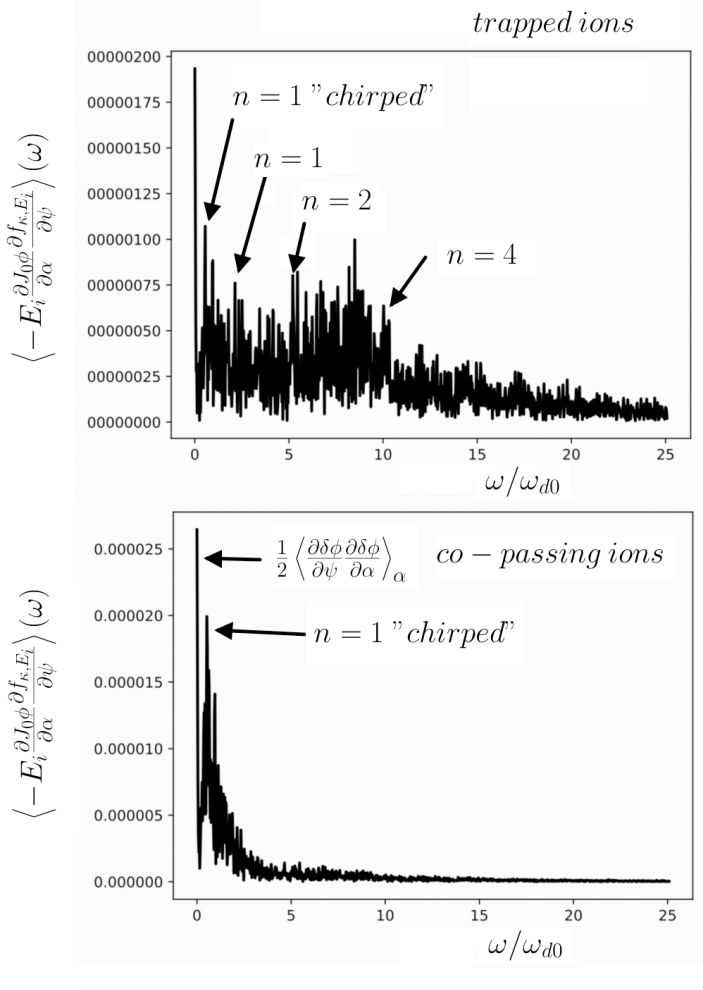


Figure 5: Illustration of the spectrum of the quantity $\langle E_i \frac{\partial J_{0i} \phi}{\partial \alpha} \frac{\partial \bar{f}_i}{\partial \psi} \rangle$, the first moment in ion energy E_i of $\frac{\partial J_{0i} \phi}{\partial \alpha} \frac{\partial \bar{f}_i}{\partial \psi}$, the average operator $\langle . \rangle$ being made on all variables κ , E_s , ψ and α . This function gives an estimation of the order parameter $\langle \Lambda_s(\psi, \alpha, t) \rangle_{\psi, \alpha}$ in the synchronization mechanism induced by the “pump” driver term (the trapped ion mode, on top panel) and another particle mode (the co-circulating ion mode in bottom panel). The different frequencies corresponding to coherent structures occurring in Fig. 4 are represented by arrows in the frequency spectrum.

had an initial frequency $\omega \sim \frac{3}{2}\omega_{d0}\overline{\omega_d}(\kappa)\frac{T_i}{T_0}$, which decreases to a value of $\omega \sim 0.5\omega_{d0}$, well below the value $\langle \frac{3}{2}\omega_{d0}\omega_{d0}\overline{\omega_d}(\kappa) \rangle_\kappa \sim 2.5\omega_{d0}$ (for $T_i = T_0$). This mode is connected to the coupling between KH and the interchange-type ITG instability, where wave-particle energy exchange can be enhanced by resonant frequency sweeping.

In conclusion, the energetic or thermal particle modes described by Vlasov equations of type (23) can be seen as a fundamental paradigm for the study of collective behaviors (synchrony) in a system formed by particles modes behaving as “oscillators”, whose frequencies are expressed in terms of pitch angles κ and energies E_i . When electrostatic fluctuations maintain wave-particle resonance by “phase-locking”, a significant frequency chirping is observed. Here it is the TIM that plays the role of the “particle mode pump” allowing other modes, in presence of shear flow and energetic beam ions, to become locked on the chirped TIM frequency close to $\omega \sim 0.5\omega_{d0}$, by a partial synchronization mechanism. It should be noted that a concept of "particle mode pump" has been initially introduced by White et al. in Ref. [36], but here this term is borrowed by analogy and extension: the notion of particle mode pump of those authors is indeed akin to the notion of "global synchronization" we will speak of in the companion article.

6 Conclusion

In this work we have studied the effects of a small population of energetic ions on ion-temperature-gradient modes which destabilize a population of charged particles (ions and electrons) trapped in the tokamak’s banana orbits. To this purpose, co-circulating and counter-circulating ion distributions have been both first implemented in the theoretical model (sec. 2). Interactions between energetic particle modes, trapped particle modes (as TIM, TEM, ...), and fluid modes such as zonal flows and KH-induced perturbations have been so investigated both theoretically (sec. 3) and numerically (sec. 5): to this purpose, the equivalence between the trapped particle model, extended to include circulating energetic ions, and a Kuramoto synchronization model has

been discussed (sec. 4), in the limit in which the synchronization of particle modes can be dubbed as "partial", since it involves only a fraction of modes. In a companion paper [30] we will show how this scenario can transit to a "global" synchronization state if the energy density of the circulating ion is large enough.

The results we have presented can be relevant to the physics of GAMs, too. As an example, synchronization of GAMs and (mesoscopic) magnetic fluctuations has been recently identified in the edge physics in tokamak experiments [9] about electron-cyclotron-resonance heating (electron-CRH). The observations reported in [9] suggest that the phase shifts between GAMs and magnetic fluctuations can be locked via nonlinear interactions with fast ions during electron-CRH heating. In this experiment, it was suggested that a different synchronization mechanism can be also responsible of the formation of low-frequency ZF, and thus, of the reduction of the turbulence level. The analytical model presented in this article could perfectly describe these experimental observations for the low-frequency ZF mode. Furthermore more recently, Ref. [24] showed the impact of energetic ions (due to ion-CRH in an ASDEX-Upgrade discharge) on plasma turbulence associated to the formation of internal transport barriers (ITB). Similar interpretation has been proposed for experimental observations in stellarators in [25]. An energy redistribution was observed between fast ions and plasma turbulence when the magnetic drift frequency was close to the frequency of the underlying ITG micro-instabilities. These observations suggest that energetic particles play a key role in the synchronization process. Again our model can also be applied to the study of turbulence suppression in the presence of energetic ions and preliminary results should soon be published.

We conclude by noting that it is of general importance to be able to describe and understand the mechanisms through which interactions among modes involved in tokamak turbulence occur, especially in connection with the analogy with the generation of "fishbones" modes. As discussed in sec. 5.3 phase synchronization processes, in which also fast ions intervene are opening up new perspectives on the modeling of these interactions. We expect that in

the future these subjects will catalyze increasing interest from the research community, especially for what concerns transition or bifurcation aspects and their implications on turbulence suppression associated to generation of internal transport barriers.

Acknowledgment

The authors are grateful to the IDRIS computational center, Orsay, France, for computer time allocation on their computers. This work was granted access to the HPC resources of IDRIS under allocations A0110504028 and A0130504028 made by GENCI. The data that support the findings of this study are available from the corresponding author upon reasonable request.

Appendix A: Derivation of frequencies in bounce-averaging formalism

We here provide details about the inclusion of passing particles in the bounce-averaged model. To this purpose, some elements of the trapped particle model are also recalled. Assuming an equilibrium magnetic field of the form

$$B = I(\psi) \nabla\varphi + \nabla\varphi \times \nabla\psi = \nabla(\varphi - q(\psi)\theta) \times \nabla\psi \quad (\text{A.1})$$

the trajectory of a particle can be written in the form (see Garbet et al. in Ref.[17]):

$$\begin{aligned} e\psi_G &= J_3 + e\hat{\psi}(\mathbf{J}, \alpha_2) \\ \theta_G &= \epsilon_c \alpha_2 + \hat{\theta}(\mathbf{J}, \alpha_2) \\ \varphi_G &= \alpha_3 + q(J_3) \hat{\theta}(\mathbf{J}, \alpha_2) + \hat{\varphi}(\mathbf{J}, \alpha_2) \end{aligned} \quad (\text{A.2})$$

In the equations above the different contributions of the components of $\boldsymbol{\alpha} = (\alpha_1, \alpha_2, \alpha_3)$ appear explicitly: α_1 is the cyclotron phase, α_2 is the bounce or transit angle (depending on whether the particle is trapped or circulating), and α_3 is related to the precession motion. In (A.2), $\epsilon_c = 1$ (0 respectively) for passing (trapped respectively) particles. The angle variables are therefore respectively related to the cyclotron frequency by $\dot{\alpha}_1 = \Omega_1 = \omega_c$; to the

bounce frequency for trapped particles ω_{bs} of species s by $\dot{\alpha}_2 = \Omega_2 = \omega_{bs}$, or to the transit frequency ω_{ti} for passing ions by $\dot{\alpha}_2 = \Omega_2 = \omega_{ti}$; and to the precession frequency by $\dot{\alpha}_3 = \Omega_3 = \omega_{ds}$. In Eqs. (A.2), $\widehat{\theta}(\mathbf{J}, \alpha_2)$ and $\widehat{\varphi}(\mathbf{J}, \alpha_2)$ are periodic functions with respect to α_2 : they respectively represent the bounce (or transit) motion and the deviation from the regular precession motion. Here, for each species s , m_s is the mass, μ_s the magnetic moment, $v_{s,G\parallel}$ the guiding center velocity. The label G indicates the guiding center: expressing the position \mathbf{x}_G in polar coordinates (r, θ) , the magnetic moment reads $\mu_s = \frac{m_s v_{s,G}^2}{2B(\mathbf{x}_G)}$. The invariant J_2 therefore corresponds to the total energy $E_s = \frac{1}{2}m_s v_{s,G\parallel}^2 + \mu_s B(\mathbf{x}_{s,G})$.

In agreement with the experimental conditions, we consider low beta values and a poloidal field B_θ much smaller than the toroidal magnetic field B_φ (strong guide field approximation). In this limit the modulus of the poloidal magnetic field is given as usual by $B_\theta(r, \theta) = B_0 b(\theta) = B_0 (1 + \varepsilon \sin^2 \frac{\theta}{2})$, where: B_0 is the minimal value of the magnetic field amplitude B_θ at $\theta = 0$; $R = R_0$ is the major radius and $r = r_0$ the minor radius of the tokamak; $\varepsilon = \frac{r_0}{R_0}$ is the tokamak inverse aspect ratio. In this configuration the poloidal flux is linked to the poloidal field by $d\psi = -B_\theta R_0 dr$ and $\frac{B_\theta}{B} = \frac{\varepsilon}{q(r)}$. Rather than working with the adiabatic invariant μ_s , a more convenient approach consists in introducing the pitch angle variable κ_s defined by the relation $\kappa_s^2 = \sin^2 \left(\frac{\theta_0}{2} \right) = \frac{1 - \varsigma_s (1 - \varepsilon)}{2\varepsilon \varsigma_s}$ where $\varsigma_s = \frac{\mu_s B_0}{E_s}$.

In order to simplify the notation hereafter we omit the label s in κ_s : particles are passing (or circulating) if $1 < \kappa < +\infty$ or trapped if $0 \leq \kappa < 1$. The parallel velocity takes then the form:

$$v_{G\parallel s} = \epsilon_{\parallel} v_s \left(\frac{2\varepsilon}{2\varepsilon + (1 - \varepsilon) \kappa^{-2}} \right)^{\frac{1}{2}} \left(1 - \kappa^{-2} \sin^2 \frac{\theta}{2} \right)^{\frac{1}{2}}, \quad (\text{A.3})$$

where $v_s = \sqrt{2E_s/m_s}$ and ϵ_{\parallel} is the sign of the parallel velocity.

Appendix A.1 Trapped particles

For trapped particles, in particular, for which $\kappa = \sin \frac{\theta_0}{2}$, it is better to introduce the change $\sin \theta' = \kappa^{-1} \sin \frac{\theta}{2}$ where the new variable θ' spans the interval $[0, \frac{\pi}{2}]$.

In Eq. (6) in sec. 2.2, the frequency $\omega_{ds}(\kappa, E_s) = \pm \frac{T_s}{T_0} \omega_{d0} \bar{\omega}_d^{(t)}(\kappa) E_s$ represents the ion precession frequency where the normalized frequency $\bar{\omega}_d^{(t)}(\kappa)$ reads

$$\bar{\omega}_d^{(t)}(\kappa) = \frac{1}{1 - \varepsilon + 2\varepsilon\kappa^2} \left[\frac{2E(\kappa)}{K(\kappa)} - 1 + 4s_0 \left(\frac{E(\kappa)}{K(\kappa)} + \kappa^2 - 1 \right) \right] \quad (\text{A.4})$$

while the bounce frequency is given by:

$$\omega_{bs} = \sqrt{\frac{2E_s}{m_s}} \frac{1}{q_0 R_0} \bar{\omega}_b^{(t)}(\kappa) \quad \text{with} \quad \bar{\omega}_b^{(t)}(\kappa) \simeq \frac{\pi\sqrt{\varepsilon}}{2\sqrt{2}K(\kappa)} \quad (\text{A.5})$$

where $s_0 = \frac{r_0}{q_0} \left(\frac{dq}{dr} \right)_{r_0}$ is the magnetic shear. $K(\kappa)$ and $E(\kappa)$ are the complete elliptic integrals of the first and second kind respectively.

Appendix A.2 Passing ions

For passing particles, by exploiting the up-down symmetry, the integrals over θ run over the interval $[0, \pi]$. It is also convenient to introduce the change $\theta' = \frac{\theta}{2}$, so to express Eq. (A.3) in terms of Elliptic functions. The variable α_3 is approximated to

$$\alpha_3 = \varphi_G - q(J_3) \hat{\theta}(\mathbf{J}, \alpha_2) - \hat{\varphi}(\mathbf{J}, \alpha_2) = \varphi_G - q_0(\psi) (\theta_G - \alpha_2) \simeq \alpha \quad (\text{A.6})$$

Finally, by making the double gyro-average over fast scales (cyclotron plus bounce or transit motion), the two main variables are the poloidal flux ψ and the precession phase $\alpha = \varphi - q_0\theta$, once we have neglected the deviation from the regular precession motion and the dependence on α_2 , after performing the gyro-average over the transit motion. To complete the analysis of the orbits, we must determine the frequencies with which the fast ion performs

their periodic motion in θ and φ . These correspond to the toroidal precession frequency and the ion transit frequency. Using the pitch-angle parameter κ (with $\kappa > 1$, here), in the large spect ratio limit we thus write:

$$\bar{\omega}_d^{(c)}(\kappa) = \frac{1}{1 - \varepsilon + 2\varepsilon\kappa^2} \left[1 + 2\kappa^2 \left(\frac{E(\kappa^{-1})}{K(\kappa^{-1})} - 1 \right) + 4s_0 \frac{E(\kappa^{-1})}{K(\kappa^{-1})} \right] \quad (\text{A.7})$$

for the precession frequency and

$$\bar{\omega}_b^{(c)}(\kappa) \simeq \frac{\pi\kappa\sqrt{\varepsilon}}{K(\kappa^{-1})} \quad (\text{A.8})$$

for the transit frequency.

Appendix B: linear analysis of trapped ion modes

Here we recall the main features of TIM turbulence (i.e. without passing ions or trapped electrons), already cited in Ref. [10]. By linearizing the Vlasov equation (7) and by assuming an adiabatic response of electrons and passing ions, the trapped ion distribution function and the electric potential can be written in the form:

$$\bar{f}_i(\psi, \alpha, t) = F_0^{(t)}(\psi) + \sum_n \delta f_n(\psi) e^{i(n\alpha - \omega t)}, \quad (\text{B.1})$$

$$\phi(\psi, \alpha, t) = \sum_n \delta\phi_n(\psi) e^{i(n\alpha - \omega t)}, \quad (\text{B.2})$$

where the initial condition for the trapped ion distribution reads

$$F_0^{(t)}(\psi) = e^{-E_i} \left[1 + \Delta\tau\omega_{d0}\bar{\omega}_d^{(t)}(\kappa) \left(E_i - \frac{3}{2} \right) \psi \right] \quad (\text{B.3})$$

and where $\Delta\tau = \frac{1}{T_i} \frac{dT_i}{d\psi}$ is the ion temperature gradient. It is possible, for collisionless TIMs, to determine the marginal solution for the electric potential fluctuations. Combining reduced Vlasov equation (7) with the quasi-neutrality condition (13) and with an adiabatic response for other species, we can write

$$C_e \delta\phi_n = \frac{2}{\sqrt{\pi}} \int_0^{+\infty} dE_i \sqrt{E_i} \int_0^1 d\kappa \kappa K(\kappa) \frac{\Delta\tau e^{-E_i} (E_i - \frac{3}{2})}{E_i - \frac{\omega}{n\omega_{d0} \frac{T_i}{T_0} \bar{\omega}_d^{(t)}(\kappa)}} J_{0i}^{(t)2} \delta\phi_n \quad (\text{B.4})$$

with the usual Landau prescription on the imaginary part of ω . In the linear regime the imaginary part of (B.4) must cancel exactly for the marginal solution, so it is possible to determine the eigenfrequencies of TIMs in the form

$$\omega_{TIM} = \frac{3}{2} n\omega_{d0} \frac{T_i}{T_0} \bar{\omega}_d^{(t)}(\kappa) \quad (\text{B.5})$$

for a population characterized by the pitch angle variable κ . It must be recalled that, in deriving the basic form of the dispersion relation (B.4) for trapped ion modes, Tang et al., in Ref. [21] retained up to ω^{-3} terms in the asymptotic expansion of the solution of Eq.(B.4). This leads to $\omega = \delta\omega + \frac{5}{2} n\omega_{d0} \bar{\omega}_d(\kappa)$ (having assumed $T_i \sim T_0$ so to simplify the calculations), whence we recognize an interchange mode with frequency $\omega_I \simeq \frac{5}{2} n\omega_{d0} \bar{\omega}_d(\kappa)$. To deal with a kinetic version of the interchange mode, the integral of (B.4) must be analytically continued, thus generating additional terms leading to $\omega_{TIM} = \omega_I + \delta\omega = \frac{5}{2} n\omega_d(\kappa) + \frac{2\varepsilon\omega_{e*}}{2(1+\tau)} \simeq \frac{3}{2} n\omega_d(\kappa)$, where ω_{e*} is the electron diamagnetic frequency and $\tau = \frac{T_e}{T_i}$. Here the correction in frequency brought by $\delta\omega$ is negative. Eq. (B.4) reduces to

$$\delta\phi_n - \frac{\Delta\tau}{C_e} \frac{2}{\sqrt{\pi}} \int_0^{+\infty} dE_i \sqrt{E_i} \int_0^1 d\kappa \kappa K(\kappa) e^{-E_i} \left(J_{0i}^{(t)} \right)^2 \delta\phi_n = 0 \quad (\text{B.6})$$

Thus, for zero boundary conditions in ψ , the eigenfunctions are given by $\delta\phi_n(\psi) = \sin(l\pi\psi)$ with $l = 0, 1, 2, \dots$. The knowledge of this marginal solution allows us to determine the threshold of the ITG-type instability: for instance for $l = 1$ and $\rho_{ci} = 0$, we have $\Delta\tau_s = \frac{C_e}{\xi}$ where $\xi = 1 - \frac{3}{4}\delta_{bi}^2 - \frac{15}{64}\delta_{bi}^4$ is close to one.

Appendix C: Kuramoto synchronization versus Landau damping

A strong correspondence can be established between the Kuramoto synchronization approach and the electrostatic limit of the Vlasov equation.

Starting from the one-dimensional slab model in the $x - v$ phase space, the Vlasov equation writes

$$\frac{\partial f}{\partial t} + v \frac{\partial f}{\partial x} + \frac{eE}{m} \frac{\partial f}{\partial v} = 0 \quad (\text{C.1})$$

and is coupled nonlinearly with the Poisson equation

$$\frac{\partial E}{\partial x} = \frac{e}{\epsilon_0} \int_{-\infty}^{+\infty} f dv - \frac{en_0}{\epsilon_0} \quad (\text{C.2})$$

Thus, by linearizing the Vlasov equation (C.1) around an homogeneous equilibrium $F_0(v)$, i.e. $f = F_0(v) + \delta f(k, v, t) e^{ikx}$, the set of Eqs. (C.1) and (C.2) leads to

$$\frac{\partial \delta f}{\partial t} + ikv \delta f(k, v, t) + \frac{e \delta E(k, t)}{m} \frac{dF_0}{dv} = 0 \quad (\text{C.3})$$

$$\text{and} \quad ik \delta E(k, t) = \frac{e}{\epsilon_0} \int_{-\infty}^{+\infty} \delta f(k, vt) dv \quad (\text{C.4})$$

Finally eliminating δE yields to

$$\frac{\partial \delta f}{\partial t} = -ikv \delta f(k, v, t) - \frac{i\omega_p^2}{kn_0} \frac{dF_0}{dv} \int_{-\infty}^{+\infty} \delta f(k, vt) dv \quad (\text{C.5})$$

which is similar to Eq. (33). Eqs. (33) and (C.5) are nonlinear integro-partial-differential equations for $\delta\rho$ and δf respectively.

References

- [1] K. Itoh, S.I. Itoh, P.H. Diamond, T.S. Hahm, A. Fujisawa, G.R. Tynan, M. yadi and Y. Nagashima, Phys. Plasmas **13**, 055502 (2006).

- [2] N. Winsor, J.L. Johnson, J.M. Dawson, Phys. Fluids **11**, 2448 (1968).
- [3] B. Scott, Phys. Letters A **320**, 53 (2003).
- [4] G.Y. Fu, Phys. Rev. Letters **101**, 185002 (2008).
- [5] D. Zarzoso, D. Del Castillo Negrete, D.F. Escande, Y. Sarazin, X. Garbet, V. Grandgirard, C. Passeron, G. Latu, S. Benkadda, Nucl Fusion **58**, 106030 (2018).
- [6] Z. Qiu, L. Chen, F. Zonca Plasma Sci. Techno. **20**, 09004 (2018).
- [7] A. Ghizzo and F. Palermo, Phys. Plasmas **22**, 082303 (2015).
- [8] A. Ghizzo and F. Palermo, Phys. Plasmas **22**, 082304 (2015).
- [9] K.J. Zhao, Y. Nagashima, P.H. Diamong, J.Q. Dong, K. Itoh, S.I. Itoh, L.W. Yang, J. Cheng, A. Fujisama, S. Inagaki, Y. Kosuga, M. Sasaki, Z.X. Wang, L. Wei, Z.H. Huang, D.L. Yu, W.Y. Hong, Q. Li, X.Q. Ji, X.M. Song, Y. Huang, Yi Liu, Q.W. Yang, X.T. Ding, X.R. Duan, Phys. Rev. Letters **117**, 145002 (2016).
- [10] G. Depret, X. Garbet, P. Bertrand, A. Ghizzo, Plas. Phys. Control. Fusion **42**, 949 (2000).
- [11] T. Cartier-Michaud, P. Ghendrih, V. Grandgirard, G. Latu, Optimizing the parallel scheme of the Poisson solver for the reduced kinetic code TERESA, ESAIM: Proceedings, 43, 274 (2013).
- [12] A. Ghizzo, D. Del Sarto, X. Garbet, Y. Sarazin, Phys. Plasmas **17**, 092501 (2010).
- [13] Y. Kuramoto, *Chemical Oscillations, Waves and Turbulence*, Springer-Verlag, Berlin (1984).
- [14] Y. Kuramoto and I. Nishikawa, J. Stat. Physics **49**, 569 (1987).
- [15] J.A. Acebron, L.L. Bonilla, C. J. Perez Vicente, F. Ritort, R. Spigler, Rev. Modern Physics **77**, 135 (2005).

- [16] T. Stankovski, T. Pereira, P. V.E. McClintock, A. Stefanovska, *Rev. Modern Physics* **89**, 045001 (2017).
- [17] X. Garbet, L. Laurent, F. Mourgues, J.P. Roubin, A. Samain, *J. Comput. Physics* **87**, 249 (1990).
- [18] B.B. Kadomtsev and O.P. Pogutse *Nucl. Fusion* **11**, 67 (1971).
- [19] L. Chen and F. Zonca, *Rev. of Modern Physics* **88**, 015008 (2016).
- [20] L. Chen and F. Zonca, *Phys. Plasmas* **20**, 055402 (2013).
- [21] W. M. Tang, P.H. Rutherford, H.P. Furth, J.C. Adam, *Phys. Rev. Letters* **35**, 660 (1975).
- [22] S.H. Strogatz, R.E. Mirollo, P.C. Matthews, *Phys. Rev. Letters* **68**, 2730 (1992).
- [23] S. Xu, Z.B. Guo, A. D. Gurcan, *Phys. Eev. E* **103**, 023208 (2021).
- [24] A. Si Siena, R. Bilato, T. Gorler, A. Banon Navarro, E. Poli, V. Bobkov, D. Jarema, E. Fable, C. Angioni, Ye O. Kazakov, R. Ochoukov, P. Schneider, M. Weiland, F. Jenko, and the ASDEX Upgrade Team, *Phys. Rev. Letters* **127**, 025002 (2021).
- [25] A. Si Siena, A. Banon Navarro, F. Jenko, *Phys. Rev. Letters* **125**, 105002 (2020).
- [26] E. Sonnendrucker, J. Roche, P. Bertrand, A. Ghizzo, *J. Comput. Physics* **149**, 201 (1999).
- [27] A. Ghizzo, P. Bertrand, M. Shoucri, E. Fijalkow, M.R. Feix, *J. Comput. Physics* **108**, 105 (1993).
- [28] P.H. Diamond, S.I. Itoh, K. Itoh *Modern Plasma physics. Vol I. Physical Kinetics of Turbulent Plasmas*, Cambridge, Cambridge University Press (2010).

- [29] A. Ghizzo and D. Del Sarto, Plasma Phys. Control. Fusion **63**, 055007 (2021).
- [30] A. Ghizzo and D. Del Sarto, *Transition to a fishbone-like state triggered by global synchronization of particle modes and energetic particles in gyrokinetic turbulence*, submitted to Phys. Plasmas.
- [31] L. Chen and F. Zonca, Nucl. Fusion **47**, S727 (2007).
- [32] F. Zonca, L. Chen, S. Briguglio, G. Fogaccia, G. Vlad, X. Wang, New J. Phys. **17**, 013052 (2015).
- [33] H.L. Berk, C.W. Nielson, K.W. Roberts, Phys. Fluids **13**, 980 (1970).
- [34] T.M. Dupree, Phys. Fluids **25**, 277 (1982).
- [35] H.L. Berk and B.N. Breizmann, Phys. Fluids B, **2**, 2226 (1990).
- [36] R.B. White, R.J. Goldston, K. McGuire, A.H. Boozer, D.A. Monticello, W. Park Phys. Fluids **26**, 2958 (1983).